IEEE Access
Multidisciplinary : Rapid Review : Open Access Journal

Received December 24, 2020, accepted January 28, 2021, date of publication February 1, 2021, date of current version February 8, 2021.

Digital Object Identifier 10.1109/ACCESS.2021.3056083

Thickness and Refractive Index Measurement System for Multilayered Samples

CHIEN-SHENG LIU, (Member, IEEE), AND TZU-YAO WENG
Department of Mechanical Engineering, National Cheng Kung University, Tainan 70101, Taiwan

Corresponding author: Chien-Sheng Liu (csliu@mail.ncku.edu.tw)

This work was supported by the Ministry of Science and Technology of Taiwan under Grant MOST105-2221-E-006-265-MY5, Grant MOST106–2628-E-006–010-MY3, and Grant MOST109–2218-E-002–006.

ABSTRACT In order to simultaneously obtain the thickness and refractive index for each layer of multilayered samples, this paper proposes a novel measurement system with a simple structure by using geometric optics. The key point of the overall structure is that the binary linear equation relation between the upper and lower planes of the layer can be known by the distances between laser spots reflected from the layer. Using two optical paths with different incident angles of laser beams, the CCD sensors capture the spot signal for image processing binarization and data sampling. After the obtained laser spots' spacing is substituted into the equations, the thicknesses and refractive indexes of the multilayered samples can be calculated and measured. The proposed measurement system is characterized numerically using simulations on the commercial software program Zemax and then experimentally tested using a laboratory-built prototype. The experiment results show that the refractive indexes and the thicknesses of three-layer samples were measured with high accuracy (with maximum measurement errors of 2.4% and 2% for a refractive index n and thickness t, respectively).

INDEX TERMS Auto-focusing microscopy, multilayered samples, optical system, refractive index, thickness.

I. INTRODUCTION

For a long time, optical technology has been an important tool for non-destructive testing [1]. Especially in recent years, the precision miniaturization of electronic products has become a mainstream trend. Production and testing equipment for component processing and assembly has also received more attention [2], [3]. How to ensure product quality control is a very important issue. In manufacturing and inspection fields, machine vision systems are increasingly used due to their reliability, relatively low cost and high throughput. It is usually necessary to focus the camera to obtain a clear image of the target object [4]–[13]. However, for the existing optics-based microscopes, they are only suitable for single layer of samples or reflected surfaces [14]–[21]. For the biomedical inspection, three-layer samples (for example, the cover glass, biological sample, and slide glass) are popular. Consequently, manual focusing microscopes are widely used and they are time consuming. Therefore, it is a critical issue to simultaneously obtain the thickness for each layer of multilayered samples to implement the auto-focusing function.

In addition, biological testing is also in greater demand due to the development of minimally invasive surgery. The development of laser therapy and other precision surgery has higher requirements for understanding the phenomenon of light transmission and refraction between biological tissues. Especially when using an optical coherence tomography system, it will affect the contrast of the image and the subsequent calculation of tissue thickness [22]–[24]. As a result, there are various measurement techniques proposed over the last decade for the simultaneous measurement of the refractive index and thickness of samples [25]–[44]. However, to the best of our knowledge, there is not any existing method to simultaneously measure the thickness and refractive index for each layer of multilayered samples.

Therefore, in this paper, the proposed measurement system was able to simultaneously obtain the thickness and refractive index for each layer of multilayered samples. The proposed measurement system was characterized numerically, after which the results were verified experimentally using a laboratory-built prototype.

The associate editor coordinating the review of this manuscript and approving it for publication was Wuliang Yin.

This work is licensed under a Creative Commons Attribution 4.0 License. For more information, see https://creativecommons.org/licenses/by/4.0/

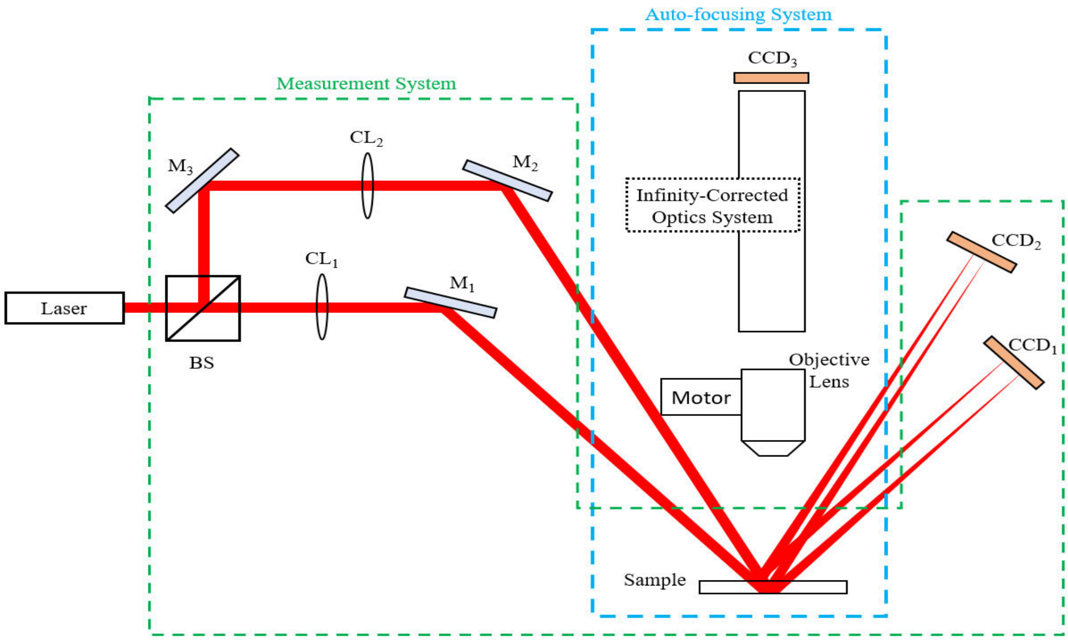

FIGURE 1. Structure of proposed measurement system.

II. PROPOSED MEASUREMENT SYSTEM WITH DIFFERENT INCIDENT ANGLES

A. STRUCTURE

The structural design of the proposed measurement system is inspired by the triangulation distance measurement. As shown in Fig. 1, two sets of reflective geometric optical architectures with different incident angles are designed for measurement. The two sets of mathematical formulas from the two different incident angles can mutually calculate the respective thickness and refractive index for each layer of multilayered samples. The proposed measurement system can be integrated into an auto-focusing system for further auto-focusing applications. In the proposed measurement system, the laser on the main optical axis is first split into two optical paths through a beam splitter (BS), and the laser beam in each optical path passes through a convex lens (CL_1, CL_2) for laser beam shaping, respectively. In order to produce two different incident angles (30° and 45°), the laser beams in two optical paths will pass through a mirror (M_1, M_2), respectively. The angles of 30° and 45° are chosen for the biomedical inspection of three-layer samples (thickness of 0.3 mm $\sim$ 2 mm) with suitable measuring accuracy. The laser beams reflected from the upper and lower surfaces of the samples will be focused on two charge-coupled devices (CCD_1 and CCD_2). Consequently, MATLAB software was used to perform the proposed digital image processing technique to simultaneously obtain the thickness and refractive index for each layer of multilayered samples. By using the thicknesses obtained by the proposed measurement system, the motor of the auto-focusing system can be controlled to move the objective lens to achieve the auto-focusing function on the target surface.

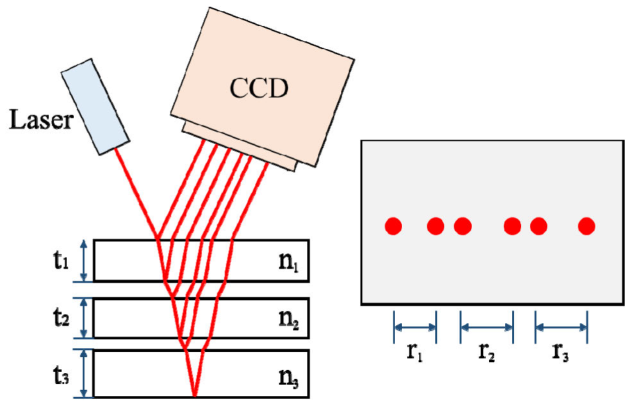

FIGURE 2. Schematic illustration of optical path in proposed measurement system.

B. MEASUREMENT PRINCIPLE

The aim of this paper is to measure the physical thickness and refractive index for each layer of multilayered samples, in special, for biomedical applications. In this paper, three-layer glasses were used to represent the cover glass, biological sample, and slide glass. When stacking three pieces of glasses, there are two air gaps between glasses. Therefore, the reflected laser spots are 6 points. The basic principle of the mathematical model proposed in this paper is shown in Fig. 2. As laser beam enters the glass sheet, it will produce both refraction and reflection. According to the principle of geometric optics, the relationship between the light spots on the CCD sensors and the thicknesses and refractive indexes of the three-layer samples can be calculated.

Since six unknowns of thicknesses and refractive indexes are required, this issue is solved with two different incident

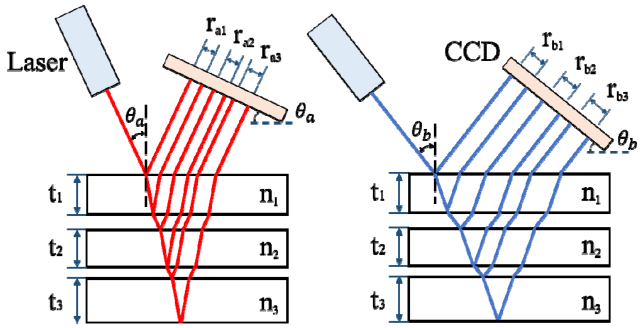

FIGURE 3. Detailed illustration of different incident angles.

angle beams, as shown in Fig. 3. According to the geometric relationship described in the figure and Snell's Law, we can get the relationship between the spot distance (r) on the CCD sensor and the refractive index (n) and thickness (t) of the sample:

$$\begin{cases} r_{a1} = 2 \cdot t_1 \cdot \tan\left[\sin^{-1}\left(\frac{\sin\theta_a}{n_1}\right)\right] \\ r_{a2} = 2 \cdot t_2 \cdot \tan\left[\sin^{-1}\left(\frac{\sin\theta_a}{n_2}\right)\right] \\ r_{a3} = 2 \cdot t_3 \cdot \tan\left[\sin^{-1}\left(\frac{\sin\theta_a}{n_3}\right)\right] \end{cases} \tag{1}$$

$$\begin{cases} r_{b1} = 2 \cdot t_1 \cdot \tan\left[\sin^{-1}\left(\frac{\sin\theta_b}{n_1}\right)\right] \\ r_{b2} = 2 \cdot t_2 \cdot \tan\left[\sin^{-1}\left(\frac{\sin\theta_b}{n_2}\right)\right] \\ r_{b3} = 2 \cdot t_3 \cdot \tan\left[\sin^{-1}\left(\frac{\sin\theta_b}{n_3}\right)\right] \end{cases} \tag{2}$$

By dividing (1) and (2), we can get:

$$\frac{r_{a1}}{r_{b1}} = \frac{\tan\left[\sin^{-1}\left(\frac{\sin\theta_a}{n_1}\right)\right]}{\tan\left[\sin^{-1}\left(\frac{\sin\theta_b}{n_1}\right)\right]} \tag{3}$$

$$\frac{r_{a2}}{r_{b2}} = \frac{\tan\left[\sin^{-1}\left(\frac{\sin\theta_a}{n_2}\right)\right]}{\tan\left[\sin^{-1}\left(\frac{\sin\theta_b}{n_2}\right)\right]} \tag{4}$$

$$\frac{r_{a3}}{r_{b3}} = \frac{\tan\left[\sin^{-1}\left(\frac{\sin\theta_a}{n_3}\right)\right]}{\tan\left[\sin^{-1}\left(\frac{\sin\theta_b}{n_3}\right)\right]} \tag{5}$$

In (3), (4) and (5), the distances and angles are known, so the refractive index of each layer can be obtained. Then the thickness can be obtained by substituting the refractive index of each layer into (1) and (2).

III. OPTICAL SIMULATION OF PROPOSED MEASUREMENT SYSTEM AND IMAGE PROCESSING PROCEDURE

In this section, a series of numerical simulations using the software program Zemax were performed to design and verify the measurement performance of the proposed measurement system. In the proposed measurement system, the convex lenses (CL_1, CL_2) are designed to shape the laser beam spot, so Zemax simulations can be used to confirm the shaping effect.

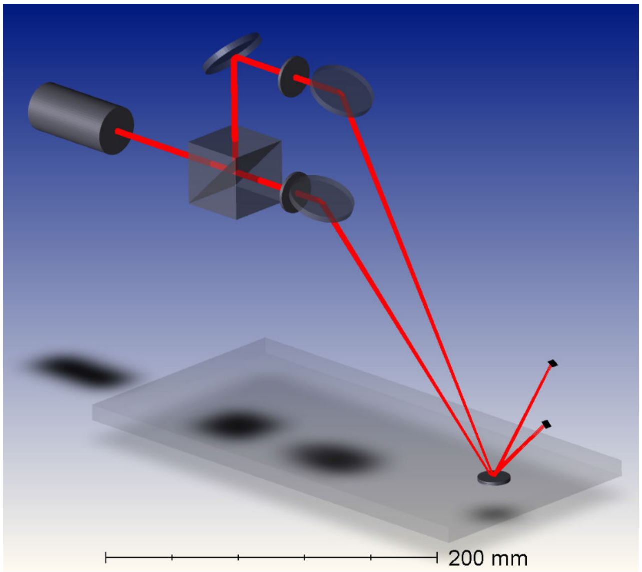

FIGURE 4. Zemax 3D optical model of proposed measurement system.

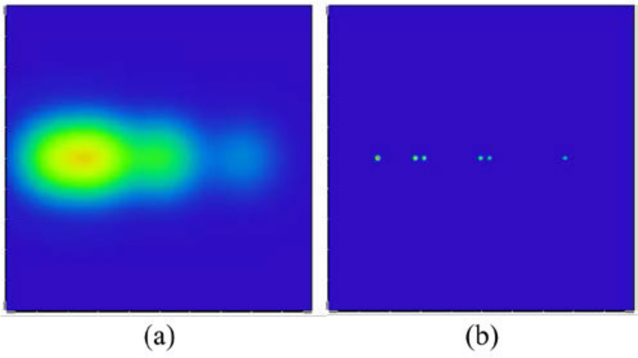

FIGURE 5. Zemax 3D optical model of proposed measurement system.

Figure 4 shows the Zemax 3D optical model of the proposed measurement system. Figures 5a and 5b show the simulated laser spots on CCD_1 without and with the convex lens, respectively. It can be clearly seen that the plastic effect obviously separates the laser spots, which improves the post-image processing efficiency. The selected design parameters of the proposed measurement system are listed in Table 1.

To determine the spot distance (r), we used the proposed digital image processing technique and MATLAB software to process and analyze images captured by the CCD sensors. The proposed digital image processing technique involves three fundamental steps: (1) image median filtering, (2) image binarization, and (3) data sampling. Figure 6 shows the original laser spot image made by Zemax; the image processing results aid in retrieving the distances between laser spots. As shown, the distances between the laser spots in the images captured by the CCDs can be calculated. A more comprehensive description of the image processing technique is provided in our previous studies [20], [45], [46].

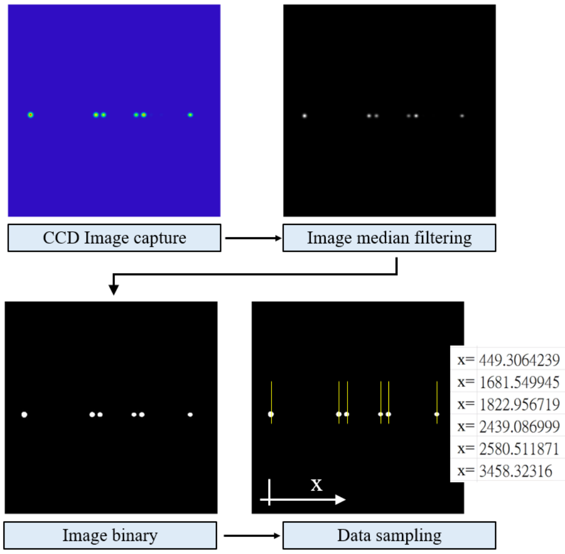

FIGURE 6. Image processing procedure and results.

TABLE 1. Design parameters of proposed measurement system.

Component	Brand	Specification
Laser	Thorlabs	HL6501MG
BS	Thorlabs	CM1-BS013(50:50)
M_1, M_2, M_3	Thorlabs	PF10-03-P01-10
CL_1	Thorlabs	LA1484, f_0=300 mm
CL_2		LA1172, f_0=400 mm
Sample	Edmund	Sapphire Window ZnSe Window Magnesium Fluoride Window
Objective Lens	Olympus	f_0=18 mm
CCD_1, CCD_2	Basler	5472*3648 (pixel), 17fps
CCD_3	Duma	1280*1024 (pixel), 50 fps
Infinity-Corrected Optics System	Navita	1-60255
Motor	PI	UPL120, 13 mm

To verify that the proposed measurement system can simultaneously measure the thicknesses and refractive indexes of three-layer samples, four common transparent materials such as sapphire, borosilicate glass (BK7), magnesium fluoride glass (MgF2), and zinc selenide glass (ZnSe) were simulated. The thickness of BK7 that represent microslide with a refractive index of 1.5168 is 0.7 mm; the thickness of MgF2 with a refractive index of 1.3777 is 2 mm; the thicknesses of sapphire with a refractive index of 1.7682 are 1mm and 2mm, respectively; and the thickness of ZnSe with a refractive index of 2.3674 is 2 mm.

Figures 7 and 8 present two sets of simulation results for the simulated image and the calculated thicknesses and refractive indexes, respectively. The first set of samples are with the upper 2 mm MgF2, the middle 1 mm sapphire, and the lower 0.7 mm BK7. The second set of samples are with the upper layer 0.7 mm BK7, the middle layer 2 mm sapphire, and the lower layer 2 mm ZnSe.

From the simulation results, the calculated thickness error and refractive index error are about 0.05% and 0.1%, respectively. Due to its low deviation value and high accuracy, the feasibility of this mathematical model and the proposed measurement system can be proved.

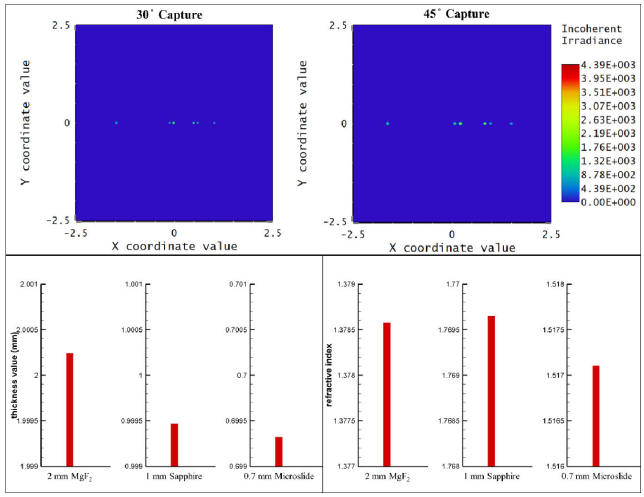

FIGURE 7. Simulation results for first set of samples.

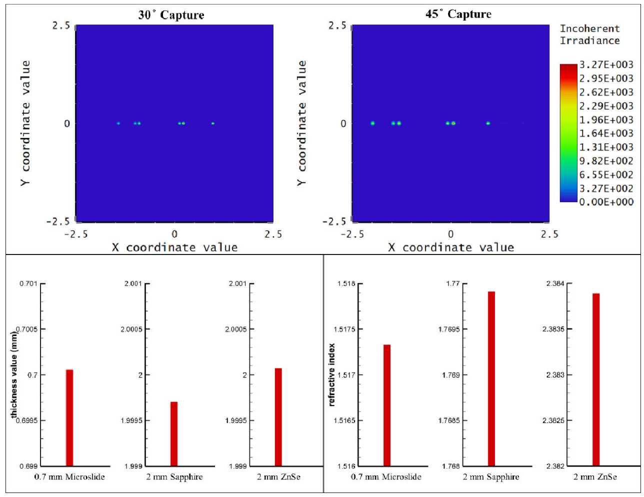

FIGURE 8. Simulation results for second set of samples.

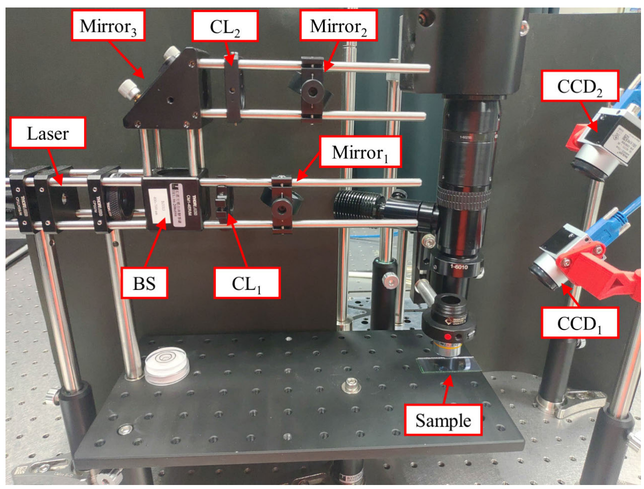

FIGURE 9. Laboratory-built prototype of proposed measurement system and sample.

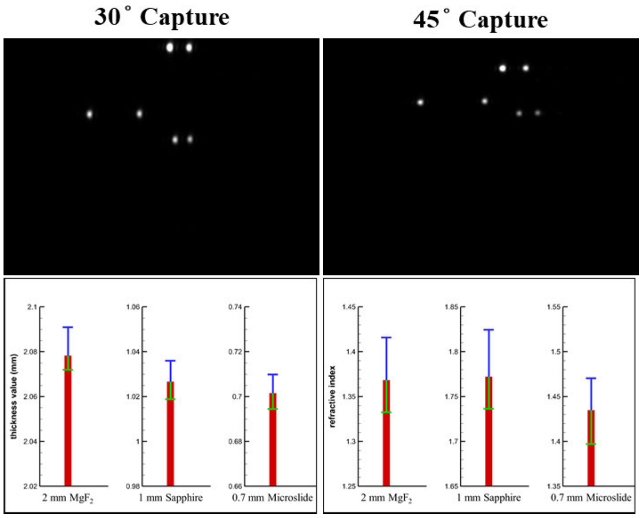

FIGURE 10. Experimental results for first set of samples.

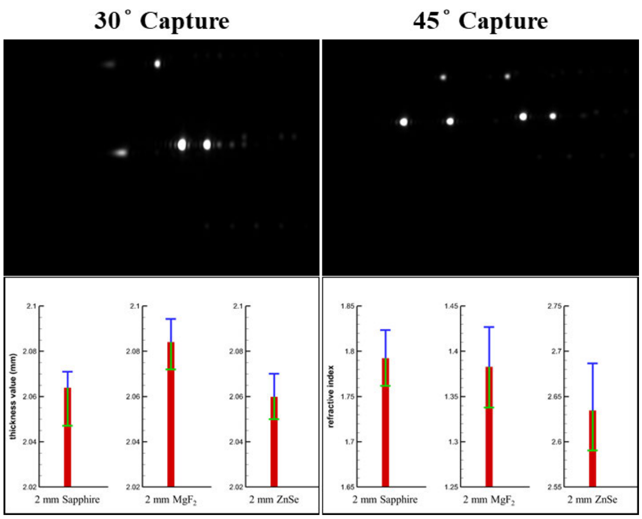

FIGURE 11. Experimental results for second set of samples.

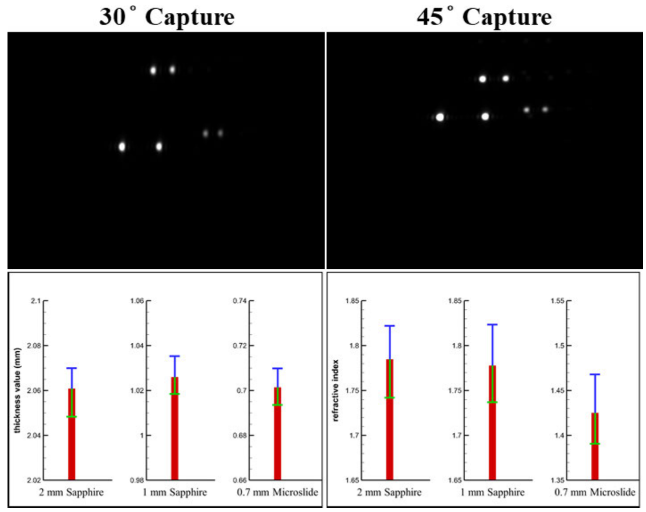

FIGURE 12. Experimental results for third set of samples.

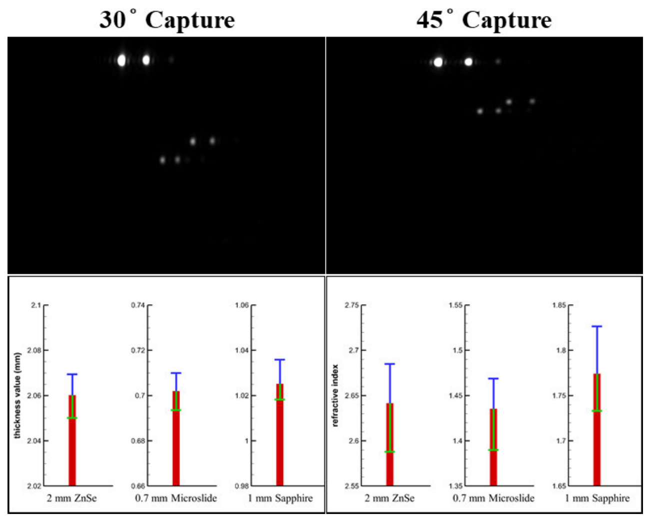

FIGURE 13. Experimental results for fourth set of samples.

IV. EXPERIMENTAL RESULTS AND DISCUSSION

The validity of the proposed measurement system was verified using a laboratory-built prototype. Figure 9 shows a photograph of the laboratory-built prototype and sample.

In this section, a total of 5 glass sheets were measured, including 4 kinds of materials, and the true thicknesses were obtained through a commercial coordinate measuring machine (CMM, ZIESS Calypso). The thickness of MgF2 with a refractive index of 1.377 is 2.079 mm; the thicknesses of sapphire with a refractive index of 1.77 are 1.029 mm and 2.052 mm, respectively; the thickness of ZnSe with a refractive index of 2.631 is 2.058 mm; and the thickness of a general glass slide of unknown material is 0.707 mm. Take three of these arrangements and measure the thicknesses and refractive indexes of three glass slides simultaneously. Figures 10 to 13 show the experimental images and measurement results of 4 sets of samples, respectively. The first set of samples are with the upper layer 2 mm MgF_2, the middle layer 1 mm sapphire, and the lower layer 0.7 mm microslide. The second set of samples are with the upper layer 2 mm sapphire, the middle layer 2 mm MgF_2, and the lower layer 2 mm ZnSe. The third set of samples are with the upper layer 2 mm sapphire, the middle layer 1 mm sapphire, and the lower layer 0.7 mm microslide. The fourth set of samples are with the upper layer 2 mm ZnSe, the middle layer 0.7 mm microslide, and the lower layer 1 mm sapphire.

From the experimental results, it can be deduced that the measured errors for thickness and refractive index in the actual experiments are about 2% and 2.4%, respectively. The errors for thickness are gotten from disparity between the measured thickness with the proposed measurement system and the measured thickness with the CMM. The errors for refractive index are gotten from disparity between the measured refractive index with the proposed measurement system

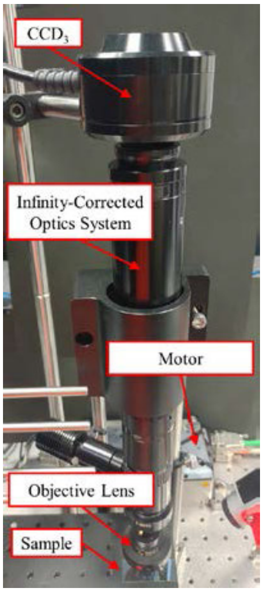

FIGURE 14. Laboratory-built prototype of auto-focusing system.

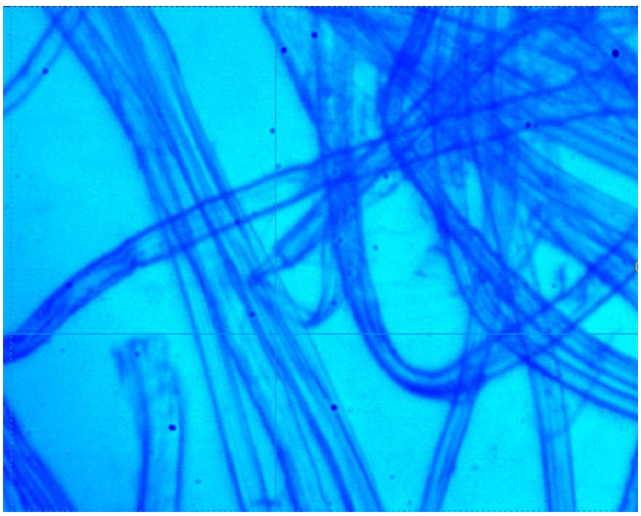

FIGURE 15. Focus image.

and the standard value with samples. The measured errors are obviously greater that the calculated errors. This is because the surface curvature (upper and lower) of each uniform refraction index layer, non-parallelism of the same optical borders in practice, and structural impurity of the layers material etc. will seriously transform the canonic application of Snell's law. As a result, the laser spots on CCD sensors are not in alignment well, as shown in Figs. 10 to 13 when comparing Figs. 7 and 8. In the future work, the non-parallelism of the samples should be considered into the proposed measurement system to improve the measuring accuracy.

Finally, the proposed measurement system was integrated into an auto-focusing system to achieve the auto-focusing function on the target surface with the three-layer samples of the upper layer 2 mm sapphire, and the middle and lower layers 0.7 mm microslides, as shown in Fig. 14. The focus target sample between each piece is scraps of lens cleaning paper. Figure 15 shows its auto-focusing image. The experimental results show that the proposed measurement system can successfully be integrated into an auto-focusing system for further biomedical application in the future.

V. CONCLUSION

This paper currently proposes an innovative, simple, and low-cost architecture for the future development of biological auto-focusing technology. It can simultaneously measure the thickness and refractive index for each layer of multilayered samples before focusing to achieve the purpose of rapid auto-focusing. The experimental results show that measured errors for thickness and refractive index are about 2% and 2.4%, respectively. Consequently, the proposed measurement system has the potential to be used in the biomedical automated inspection.

REFERENCES

[1] S. Srisuwan, C. Sirisathitkul, and S. Danworaphong, "Validiation of photometric ellipsometry for refractive index and thickness measurements," *MAPAN*, vol. 30, no. 1, pp. 31–36, Mar. 2015.

[2] G. Coppola, P. Ferraro, M. Iodice, and S. De Nicola, "Method for measuring the refractive index and the thickness of transparent plates with a lateral-shear, wavelength-scanning interferometer," *Appl. Opt.*, vol. 42, no. 19, p. 3882, Jul. 2003.

[3] A. Z. Evmenova, V. Odarych, and M. V. Vuichyk, "Ellipsometric investigation of CdTe films," *Appl. Opt.*, vol. 42, no. 3, pp. 667–675, 2012.

[4] P. Petruck, R. Riesenberg, and R. Kowarschik, "Optimized coherence parameters for high-resolution holographic microscopy," *Appl. Phys. B, Lasers Opt.*, vol. 106, no. 2, pp. 339–348, Feb. 2012.

[5] Z. Zhang, Q. Feng, Z. Gao, C. Kuang, C. Fei, Z. Li, and J. Ding, "A new laser displacement sensor based on triangulation for gauge real-time measurement," *Opt. Laser Technol.*, vol. 40, no. 2, pp. 252–255, Mar. 2008.

[6] W.-Y. Hsu, C.-S. Lee, P.-J. Chen, N.-T. Chen, F.-Z. Chen, Z.-R. Yu, C.-H. Kuo, and C.-H. Hwang, "Development of the fast astigmatic autofocus microscope system," *Meas. Sci. Technol.*, vol. 20, no. 4, Apr. 2009, Art. no. 045902.

[7] S. B. Andersson, "A nonlinear controller for three-dimensional tracking of a fluorescent particle in a confocal microscope," *Appl. Phys. B, Lasers Opt.*, vol. 104, no. 1, pp. 161–173, Jul. 2011.

[8] J. G. Ritter, R. Veith, J. P. Siebrasse, and U. Kubitscheck, "High-contrast single-particle tracking by selective focal plane illumination microscopy," *Opt. Exp.*, vol. 16, pp. 7142–7152, May 2008.

[9] L. H. I. Lim and D. Yang, "High-precision XY stage motion control of industrial microscope," *IEEE Trans. Ind. Electron.*, vol. 66, no. 3, pp. 1984–1992, Mar. 2019.

[10] P. Sripolsaen, P. Mittrapiyanuruk, and P. Keawtrakulpong, "A high speed autofocusing system for micro system applications," *J. Electron. Sci. Technol.*, vol. 14, no. 1, pp. 73–79, 2016.

[11] L. Luo, D. Xu, Z. Zhang, and J. Zhang, "Autofocusing method of microscope vision system for columnar microparts," *Comput. Eng. Appl.*, vol. 50, no. 8, pp. 122–126, 2014.

[12] S. Liu, D. Xu, F. Liu, D. P. Zhang, and Z. T. Zhang, "Relative pose estimation for alignment of long cylindrical components based on microscopic vision," *IEEE Trans. Mechatronics*, vol. 21, no. 3, pp. 1388–1399, Jun. 2016.

[13] S. Liu, D. Xu, D. Zhang, and Z. Zhang, "High precision automatic assembly based on microscopic vision and force information," *IEEE Trans. Autom. Sci. Eng.*, vol. 13, no. 1, pp. 382–393, Jan. 2016.

[14] C.-M. Jan, C.-S. Liu, and J.-Y. Yang, "Implementation and optimization of a dual-confocal autofocusing system," *Sensors*, vol. 20, no. 12, p. 3479, Jun. 2020.

[15] C.-S. Liu, R.-C. Song, and S.-J. Fu, "Design of a laser-based autofocusing microscope for a sample with a transparent boundary layer," *Appl. Phys. B, Lasers Opt.*, vol. 125, no. 11, p. 199, Nov. 2019.

[16] S. Liu and Y.-F. Li, ''Precision 3-D motion tracking for binocular microscopic vision system,'' *IEEE Trans. Ind. Electron.*, vol. 66, no. 12, pp. 9339–9349, Dec. 2019.
[17] C.-S. Liu, Z.-Y. Wang, and Y.-C. Chang, ''Design and characterization of high-performance autofocusing microscope with zoom in/out functions,'' *Appl. Phys. B, Lasers Opt.*, vol. 121, no. 1, pp. 69–80, Oct. 2015.
[18] C.-S. Liu and S.-H. Jiang, ''Precise autofocusing microscope with rapid response,'' *Opt. Lasers Eng.*, vol. 66, pp. 294–300, Mar. 2015.
[19] C.-S. Liu and S.-H. Jiang, ''Design and experimental validation of novel enhanced-performance autofocusing microscope,'' *Appl. Phys. B, Lasers Opt.*, vol. 117, no. 4, pp. 1161–1171, Dec. 2014.
[20] C.-S. Liu, Y.-C. Lin, and P.-H. Hu, ''Design and characterization of precise laser-based autofocusing microscope with reduced geometrical fluctuations,'' *Microsyst. Technol.*, vol. 19, no. 11, pp. 1717–1724, Nov. 2013.
[21] C.-S. Liu, P.-H. Hu, and Y.-C. Lin, ''Design and experimental validation of novel optics-based autofocusing microscope,'' *Appl. Phys. B, Lasers Opt.*, vol. 109, no. 2, pp. 259–268, Nov. 2012.
[22] G. J. Tearney, M. E. Brezinski, B. E. Bouma, M. R. Hee, J. F. Southern, and J. G. Fujimoto, ''Determination of the refractive index of highly scattering human tissue by optical coherence tomography,'' *Opt. Lett.*, vol. 20, no. 21, p. 2258, Nov. 1995.
[23] M. A. Ghita, C. Caruntu, A. E. Rosca, H. Kaleshi, A. Caruntu, L. Moraru, A. O. Docea, S. Zurac, D. Boda, M. Neagu, D. A. Spandidos, and A. M. Tsatsakis, ''Reflectance confocal microscopy and dermoscopy for *in vivo*, non-invasive skin imaging of superficial basal cell carcinoma,'' *Oncol. Lett.*, vol. 11, no. 5, pp. 3019–3024, May 2016.
[24] T. Fukano and I. Yamaguchi, ''Simultaneous measurement of thicknesses and refractive indices of multiple layers by a low-coherence confocal interference microscope,'' *Opt. Lett.*, vol. 21, no. 23, p. 1942, Dec. 1996.
[25] S. Kim, J. Na, M. J. Kim, and B. H. Lee, ''Simultaneous measurement of refractive index and thickness by combining low-coherence interferometry and confocal optics,'' *Opt. Exp.*, vol. 16, no. 8, pp. 5516–5526, 2008.
[26] W.-C. Kuo, Y.-K. Bou, and C.-M. Lai, ''Simultaneous measurement of refractive index and thickness of transparent material by dual-beam confocal microscopy,'' *Meas. Sci. Technol.*, vol. 24, no. 7, Jul. 2013, Art. no. 075003.
[27] K. Watanabe, M. Ohshima, and T. Nomura, ''Simultaneous measurement of refractive index and thickness distributions using low-coherence digital holography and vertical scanning,'' *J. Opt.*, vol. 16, no. 4, Apr. 2014, Art. no. 045403.
[28] J. Yao, J. Huang, P. Meemon, M. Ponting, and J. P. Rolland, ''Simultaneous estimation of thickness and refractive index of layered gradient refractive index optics using a hybrid confocal-scan swept-source optical coherence tomography system,'' *Opt. Exp.*, vol. 23, no. 23, pp. 30149–30164, 2015.
[29] R. Ma, L. Ji, and T. Yan, ''Laser multi-focus precision cutting of thick sapphire by spherical aberration rectification,'' *Opt. Lasers Eng.*, vol. 126, Mar. 2020, Art. no. 105876.
[30] T. Fukano and I. Yamaguchi, ''Separation of measurement of the refractive index and the geometrical thickness by use of a wavelength-scanning interferometer with a confocal microscope,'' *Appl. Opt.*, vol. 38, no. 19, pp. 4065–4073, 1999.
[31] S. A. Reza and M. Qasim, ''Nonbulk motion system for simultaneously measuring the refractive index and thickness of a sample using tunable optics and spatial signal processing-based Gaussian beam imaging,'' *Appl. Opt.*, vol. 55, no. 2, pp. 368–378, 2016.
[32] B. Hussain, M. Nawaz, M. Ahmed, and M. Yasin Akhtar Raja, ''Measurement of thickness and refractive index using femtosecond and terahertz pulses,'' *Laser Phys. Lett.*, vol. 10, no. 5, May 2013, Art. no. 055301.
[33] S. Srisuwan, C. Sirisathitkul, and S. Danworaphong, ''Validiation of photometric ellipsometry for refractive index and thickness measurements,'' *MAPAN-J. Metrol. Soc. India*, vol. 30, no. 1, pp. 31–36, Mar. 2015.
[34] C.-S. Liu, T.-Y. Wang, and Y.-T. Chen, ''Novel system for simultaneously measuring the thickness and refractive index of a transparent plate with two optical paths,'' *Appl. Phys. B, Lasers Opt.*, vol. 124, no. 9, Sep. 2018.
[35] S. C. Zilio, ''Simultaneous thickness and group index measurement with a single arm low-coherence interferometer,'' *Opt. Exp.*, vol. 22, no. 22, pp. 27392–27397, 2014.
[36] P. Balling, P. Mašika, P. Křen, and M. Doležal, ''Length and refractive index measurement by Fourier transform interferometry and frequency comb spectroscopy,'' *Meas. Sci. Technol.*, vol. 23, no. 9, Sep. 2012, Art. no. 094001.
[37] M. R. Jafarfard, S. Moon, B. Tayebi, and D. Y. Kim, ''Dual-wavelength diffraction phase microscopy for simultaneous measurement of refractive index and thickness,'' *Opt. Lett.*, vol. 39, no. 10, p. 2908, 2014.
[38] M. Muth, R. P. Schmid, and K. Schnitzlein, ''Ellipsometric study of molecular orientations of thermomyces lanuginosus lipase at the air–water interface by simultaneous determination of refractive index and thickness,'' *Colloids Surf. B, Biointerfaces*, vol. 140, pp. 60–66, Apr. 2016.
[39] D. Pristinski, V. Kozlovskaya, and S. A. Sukhishvili, ''Determination of film thickness and refractive index in one measurement of phase-modulated ellipsometry,'' *J. Opt. Soc. Amer. A, Opt. Image Sci.*, vol. 23, no. 10, pp. 2639–2644, 2006.
[40] C.-H. Liu, C.-C. Liu, and W.-C. Huang, ''Application of astigmatic method and snell's law on the thickness and refractive index measurement of a transparent plate,'' *Microsyst. Technol.*, vol. 19, no. 11, pp. 1761–1766, Nov. 2013.
[41] H. Wu, F. Zhang, T. Liu, and X. Qu, ''Glass thickness and index measurement using optical sampling by cavity tuning,'' *Appl. Opt.*, vol. 55, no. 34, p. 9756, 2016.
[42] D. Wang, N. Jin, L. Zhai, and Y. Ren, ''Measurement of liquid film thickness using distributed conductance sensor in multiphase slug flow,'' *IEEE Trans. Ind. Electron.*, vol. 67, no. 10, pp. 8841–8850, Oct. 2020.
[43] C.-T. Hsiung and C.-S. Huang, ''Refractive index sensor based on gradient waveguide thickness guided-mode resonance filter,'' *IEEE Sensors Lett.*, vol. 2, no. 4, pp. 1–4, Dec. 2018.
[44] M. Khodadadi, S. M. M. Moshiri, and N. Nozhat, ''Theoretical analysis of a simultaneous graphene-based circular plasmonic refractive index and thickness bio-sensor,'' *IEEE Sensors J.*, vol. 20, no. 16, pp. 9114–9123, Aug. 2020.
[45] S. Ko, C. S. Liu, and Y. C. Lin, ''Optical inspection system with tunable exposure unit for micro-crack detection in solar wafers,'' *Optik*, vol. 124, no. 19, pp. 4030–4035, 2013.
[46] C. M. Jan, C. S. Liu, C. L. Chen, and Y. T. Chen, ''Optical interference system for simultaneously measuring refractive index and thickness of slim transparent plate,'' *Opt. Lasers Eng.*, 2020.

CHIEN-SHENG LIU (Member, IEEE) received the B.S. and M.S. degrees from the Department of Power Mechanical Engineering, National Tsing Hua University, Hsinchu, Taiwan, in 1996 and 1999, respectively, and the Ph.D. degree from the Department of Mechanical Engineering, National Cheng Kung University, Tainan, Taiwan, in 2010. From 2003 to 2011, he worked with the Industrial Technology Research Institute (ITRI), Taiwan, as a Mechanical Design Engineer. From 2011 to 2012, he was an Assistant Professor with the Department of Mechanical Engineering, National Central University, Jhongli, Taiwan. In 2012, he joined the Department of Mechanical Engineering, National Chung Cheng University, Chiayi, Taiwan. Since 2018, he has been a Professor with the Department of Mechanical Engineering, National Cheng Kung University. His current research interests include applications of force sensors, voice coil motors, precision measurement, laser-based auto-focusing module, and opto-electronics sensing.

TZU-YAO WENG received the B.S. degree from the Department of Mechanical Engineering, National Central University, Taoyuan, Taiwan, in 2018, and the M.S. degree from the Department of Mechanical Engineering, National Cheng Kung University, Tainan, Taiwan, in 2020. His research interests include laser-based auto-focusing module, digital control, and mechanism design.